*Inorg. Chem.* **2007**, *46*, 10810–10818


# A Fourth Isolated Oxidation Level of the $[Mn_{12}O_{12}(O_2CR)_{16}(H_2O)_4]$ Family of Single-Molecule Magnets

**Rashmi Bagai and George Christou***

*Contribution from the Department of Chemistry, University of Florida, Gainesville, Florida 32611-7200*

Received August 7, 2007

The $Mn_{12}$ family of single-molecule magnets (SMMs) has been extended to a fourth isolated member. $[Mn_{12}O_{12}(O_2CR)_{16}(H_2O)_4]$ (**1**) exhibits three quasi-reversible one-electron-reduction processes at significantly higher potentials than $[Mn_{12}O_{12}(O_2CMe)_{16}(H_2O)_4]$. This has allowed the previous generation and isolation of the one- and two-electron-reduced versions of **1** to now be extended to the three-electron-reduced complex. For cation consistency and better comparisons, the complete series of complexes has been prepared with $NPr^n_4{}^+$ counterions. Thus, complex **1** was treated with 1, 2, and 3 equiv of $NPr^n_4I$, and this led to the successful isolation of $(NPr^n_4)[Mn_{12}O_{12}(O_2CCHCl_2)_{16}(H_2O)_4]$ (**2**), $(NPr^n_4)_2[Mn_{12}O_{12}(O_2CCHCl_2)_{16}(H_2O)_4]$ (**3**), and $(NPr^n_4)_3[Mn_{12}O_{12}(O_2CCHCl_2)_{16}(H_2O)_4]$ (**4**), respectively. Another three-electron-reduced analogue $(NMe_4)_3[Mn_{12}O_{12}(O_2CCHCl_2)_{16}(H_2O)_4]$ (**5**) was prepared by the addition of 3 equiv of $NMe_4I$ to **1**. Direct current magnetization data were collected on dried microcrystalline samples of **2**–**5** and were fit by matrix diagonalization methods to give $S = {}^{19}/_2$, $D = -0.35$ cm$^{-1}$, and $g = 1.95$ for **2**; $S = 10$, $D = -0.28$ cm$^{-1}$, and $g = 1.98$ for **3**; $S = {}^{17}/_2$, $D = -0.25$ cm$^{-1}$, and $g = 1.91$ for **4**; and $S = {}^{17}/_2$, $D = -0.23$ cm$^{-1}$, and $g = 1.90$ for **5**, where $D$ is the axial zero-field splitting parameter. Thus, the $[Mn_{12}]^{3-}$ complexes **4** and **5** possess significantly decreased absolute magnitudes of both $S$ and $D$ as a result of the three-electron addition to **1**, which has $S = 10$ and $D = -0.45$ cm$^{-1}$. The $D$ value of the series **1**–**4**/**5** shows a monotonic decrease with electron addition that is consistent with the progressive loss of $Mn^{III}$ ions, which are the primary source of the molecular anisotropy. Nevertheless, when studied by ac susceptibility techniques, the $[Mn_{12}]^{3-}$ complexes still exhibit frequency-dependent out-of-phase susceptibility signals at $\leq$2.5 K, indicating them to be single-molecule magnets (SMMs), albeit at lower temperatures compared with **1** (6–8 K range), **2** (4–6 K range), and **3** (2–4 K range); the shifts to lower temperatures reflect the decreasing $S$ and $D$ values upon successive reduction and hence the decreasing energy barrier to magnetization relaxation. Thus, the $[Mn_{12}]^{3-}$ complexes represent a fourth isolated oxidation level of the $Mn_{12}$ family of SMMs, by far the largest range of oxidation levels yet encountered within single-molecule magnetism.

## Introduction

Single-molecule magnets (SMMs) are molecules that possess a significant barrier (vs $kT$) to reorientation of their magnetization (magnetic moment) vector as a result of the combination of a large ground-state spin ($S$) and Ising (easy-axis) magnetoanisotropy (negative axial zero-field splitting parameter ($D$).[1] As such, they represent a molecular (bottom-up) approach to nanomagnetism. The first SMM was $[Mn_{12}O_{12}(O_2CMe)_{16}(H_2O)_4]\cdot 2HO_2CMe\cdot 4H_2O$[2] ($Mn_{12}$−Ac; $Mn^{IV}_4Mn^{III}_8$), and many more have since been synthesized.[3] Although complexes displaying SMM behavior are known for a variety of 3d, 4d, 4f, and mixed-metal complexes,[4,5] manganese carboxylate clusters have proven to be the most fruitful source of SMMs.[3a,b,6] With the use of only a limited palette of ligands and starting materials, a wide range of Mn SMMs has been obtained with nuclearities ranging from 2

* To whom correspondence should be addressed. E-mail: christou@chem.ufl.edu. Phone: (352) 392-8314. Fax: (352) 392-8757.

(1) Christou, G.; Gatteschi, D.; Hendrickson, D. N.; Sessoli, R. *MRS Bull.* **2000**, *25*, 66.

(2) (a) Sessoli, R.; Gatteschi, D.; Caneschi, A.; Novak, M. A. *Nature* **1993**, *365*, 141. (b) Sessoli, R.; Ysai, H.-L.; Schake, A. R.; Wang, S.; Vincent, J. B.; Folting, K.; Gatteschi, D.; Christou, G.; Hendrickson, D. N. *J. Am. Chem. Soc.* **1993**, *115*, 1804. (c) Caneschi, A.; Gatteschi, D.; Sessoli, R.; Barra, A. L.; Brunel, L. C.; Guillot, M. *J. Am. Chem. Soc.* **1991**, *113*, 5873.



10.1021/ic7015758 CCC: $37.00 
Published on Web 11/10/2007

to 84.[7] Among the known Mn SMMs, the $Mn_{12}$ family continues to be attractive for study as a result of its ease of preparation, stability, ready modification in a variety of ways, high ground-state spin ($S = 10$) and anisotropy, and the access to derivatives that crystallize in high-symmetry (tetragonal) space groups.[8]

The various modifications of the $Mn_{12}$ family of SMMs that have been accomplished to date have proven extremely useful for a myriad of reasons and studies and have permitted advances in our knowledge and understanding of $Mn_{12}$ complexes and the SMM phenomenon in general. In this regard, carboxylate substitution[9] represented a big step forward because it provided an extremely useful and convenient means of accessing other carboxylate analogues, which provided benefits such as isotopic labeling, tunability of redox properties, and increased solubility in a variety of organic solvents. One of the most informative impacts of the latter two points was the observation of multiple, reversible redox processes and the subsequent generation and isolation of one-electron-reduced complexes, i.e., salts of the $[Mn_{12}O_{12}(O_2CR)_{16}(H_2O)_4]^-$ anion, abbreviated as $[Mn_{12}]^-$.[10] The crystal structures of such salts revealed minimal change to the structure on reduction, with the added electron localized on an outer, formerly $Mn^{III}$ atom giving a trapped-valence $Mn^{IV}{}_4Mn^{III}{}_7Mn^{II}$ situation.[10] The $[Mn_{12}]^-$ salts allowed an assessment of the structural, magnetic, and spectroscopic consequences of changing the electron count, as well as allowing the study of the differences in quantum properties due to the integer vs half-integer $S$ value, since $[Mn_{12}]^-$ salts have an $S = 9\ ^1/_2$ ground state.[10−12] The subsequent introduction of carboxylates with more electron-withdrawing substituents into the $Mn_{12}$ complexes made two-electron reduction easier and led to the successful generation and isolation of two-electron-reduced $[Mn_{12}O_{12}(O_2CR)_{16}(H_2O)_4]^{2-}$ complexes, $[Mn_{12}]^{2-}$, such as salts of $[Mn_{12}O_{12}(O_2CCHCl_2)_{16}(H_2O)_4]$.[13] The $[Mn_{12}]^{2-}$ anion was again found to be of trapped-valence type, with a $Mn^{IV}{}_4Mn^{III}{}_6Mn^{II}{}_2$ oxidation state


(3) (a) Christou, G. *Polyhedron* **2005**, *24*, 2065. (b) Aromi, G.; Brechin, E. K. *Struct. Bonding* **2006**, *122*, 1. (c) Beltran, L. M. C.; Long, J. R. *Acc. Chem. Res.* **2005**, *38*, 325. (d) Rebilly, J. N.; Mallah, T. *Struct. Bonding* **2006**, *122*, 103.

(4) (a) Berlinguette, C. P.; Vaughn, D.; Canada-Vilalta, C.; Galan-Mascaros, J. R.; Dunbar, K. R. *Angew. Chem., Int. Ed.* **2003**, *42*, 1523. (b) Moragues-Canovas, M.; Riviere, P.; Ricard, L.; Paulsen, C.; Wernsdorfer, W.; Rajaraman, G.; Brechin, E. K.; Mallah, T. *Adv. Mater.* **2004**, *16*, 1101. (c) Barra, A. L.; Caneschi, A.; Cornia, A.; de Biani, F. F.; Gatteschi, D.; Sangregorio, C.; Sessoli, R.; Sorace, L. *J. Am. Chem. Soc.* **1999**, *121*, 5302. (d) Gatteschi, D.; Sessoli, R.; Cornia, A. *Chem. Commun.* **2000**, 725. (e) Benelli, C.; Cano, J.; Journaux, Y.; Sessoli, R.; Solan, G. A.; Winpenny, R. E. P. *Inorg. Chem.* **2001**, *40*, 188. (f) Boudalis, A. K.; Donnadieu, B.; Nastopoulos, V.; Clemente-Juan, J. M.; Mari, A.; Sanakis, Y.; Tuchagues, J. P.; Perlepes, S. P. *Angew. Chem., Int. Ed.* **2004**, *43*, 2266. (g) Oshio, H.; Hoshino, N.; Ito, T.; Nakano, M. *J. Am. Chem. Soc.* **2004**, *126*, 8805. (h) Aromi, G.; Aubin, S. M. J.; Bolcar, M. A.; Christou, G.; Eppley, H. J.; Folting, K.; Hendrickson, D. N.; Huffman, J. C.; Squire, R. C.; Tsai, H. L.; Wang, S.; Wemple, M. W. *Polyhedron* **1998**, *17*, 3005. (i) Price, D. J.; Batten, S. R.; Moubaraki, B.; Murray, K. S. *Chem. Commun.* **2002**, 762. (j) Dendrinou-Samara, C.; Alexiou, M.; Zaleski, C. M.; Kampf, J. W.; Kirk, M. L.; Kessissoglou, D. P.; Pecoraro, V. L. *Angew. Chem., Int. Ed.* **2003**, *42*, 3763. (k) Milios, C. J.; Raptopoulou, C. P.; Terzis, A.; Lloret, F.; Vicente, R.; Perlepes, S. P.; Escuer, A. *Angew. Chem., Int. Ed.* **2004**, *43*, 210. (l) Soler, M.; Wernsdorfer, W.; Folting, K.; Pink, M.; Christou, G. *J. Am. Chem. Soc.* **2004**, *126*, 2156−2165. (m) Koizumi, S.; Nihei, M.; Nakano, M.; Oshio, H. *Inorg. Chem.* **2005**, *44*, 1208. (n) Maheswaran, S.; Chastanet, G.; Teat, S. J.; Mallah, T.; Sessoli, R.; Wernsdorfer, W.; Winpenny, R. E. P. *Angew. Chem., Int. Ed.* **2005**, *44*, 5044. (o) Godbole, M. D.; Roubeau, O.; Mills, A. M.; Kooijman, H.; Spek, A. L.; Bouwman, E. *Inorg. Chem.* **2006**, *45*, 6713. (p) Li, Y. G.; Wernsdorfer, W.; Clerac, R.; Hewitt, I. J.; Anson, C. E.; Powell, A. K. *Inorg. Chem.* **2006**, *45*, 2376.

(5) (a) Ishikawa, N.; Sugita, M.; Wernsdorfer, W. *Angew. Chem., Int. Ed.* **2005**, *44*, 2931. (b) Mori, F.; Nyui, T.; Ishida, T.; Nogami, T.; Choi, K. Y.; Nojiri, H. *J. Am. Chem. Soc.* **2006**, *128*, 1440. (c) Costes, J. P.; Auchel, M.; Dahan, F.; Peyrou, V.; Shova, S.; Wernsdorfer, W. *Inorg. Chem.* **2006**, *45*, 1924. (d) Hamamatsu, T.; Yabe, K.; Towatari, M.; Osa, S.; Matsumoto, N.; Re, N.; Pochaba, A.; Mrozinski, J.; Gallani, J. L.; Barla, A.; Imperia, P.; Paulsen, C.; Kappler, J. P. *Inorg. Chem.* **2007**, *46*, 4458. (e) Zaleski, C. M.; Kampf, J. W.; Mallah, T.; Kirk, M. L.; Pecoraro, V. L. *Inorg. Chem.* **2007**, *46*, 1954. (f) Pointillart, F.; Bernot, K.; Sessoli, R.; Gatteschi, D. *Chem. Eur. J.* **2007**, *13*, 1602. (g) Mishra, A.; Wernsdorfer, W.; Parsons, S.; Christou, G.; Brechin, E. K. *Chem. Commun.* **2005**, 2086. (h) Mishra, A.; Wernsdorfer, W.; Abboud, K. A.; Christou, G. *J. Am. Chem. Soc.* **2004**, *126*, 15648. (i) Oshio, H.; Nihei, M.; Yoshida, A.; Nojiri, H.; Nakano, M.; Yamaguchi, A.; Karaki, Y.; Ishimoto, H. *Chem. Eur. J.* **2005**, *11*, 843. (j) Oshio, H.; Nihei, M.; Koizumi, S.; Shiga, T.; Nojiri, H.; Nakano, M.; Shirakawa, N.; Akatsu, M. *J. Am. Chem. Soc.* **2005**, *127*, 4568. (k) Martinez-Lillo, J.; Armentano, D.; De Munno, G.; Wernsdorfer, W.; Julve, M.; Lloret, F.; Faus, J. *J. Am. Chem. Soc.* **2006**, *128*, 14218. (l) Schelter, E. J.; Prosvirin, A. V.; Dunbar, K. R. *J. Am. Chem. Soc.* **2004**, *126*, 15004. (m) Sokol, J. J.; Hee, A. G.; Long, J. R. *J. Am. Chem. Soc.* **2002**, *124*, 7656. (n) Li, D. F.; Parkin, S.; Wang, G. B.; Yee, G. T.; Clerac, R.; Wernsdorfer, W.; Holmes, S. M. *J. Am. Chem. Soc.* **2006**, *128*, 4214. (o) Tang, J. K.; Hewitt, I.; Madhu, N. T.; Chastanet, G.; Wernsdorfer, W.; Anson, C. E.; Benelli, C.; Sessoli, R.; Powell, A. K. *Angew. Chem., Int. Ed.* **2006**, *45*, 1729.

(6) Brechin, E. K. *Chem. Commun.* **2005**, 5141.

(7) (a) Miyasaka, H.; Clerac, R.; Wernsdorfer, W.; Lecren, L.; Bonhomme, C.; Sugiura, K.; Yamashita, M. *Angew. Chem., Int. Ed.* **2004**, *43*, 2801. (b) Stamatatos, T. C.; Foguet-Albiol, D.; Stoumpos, C. C.; Raptopoulou, C. P.; Terzis, A.; Wernsdorfer, W.; Perlepes, S. P.; Christou, G. *J. Am. Chem. Soc.* **2005**, *127*, 15380. (c) Rajaraman, G.; Sanudo, E. C.; Helliwell, M.; Piligkos, S.; Wernsdorfer, W.; Christou, G.; Brechin, E. K. *Polyhedron* **2005**, *24*, 2450. (d) Soler, M.; Rumberger, E.; Folting, K.; Hendrickson, D. N.; Christou, G. *Polyhedron* **2001**, *20*, 1365. (e) Stamatatos, Th. C.; Abboud, K. A.; Wernsdorfer, W.; Christou, G. *Angew. Chem., Int. Ed.* **2007**, *46*, 884. (f) Ako, A. M.; Hewitt, I. J.; Mereacre, V.; Clerac, R.; Wernsdorfer, W.; Anson, C. E.; Powell, A. K. *Angew. Chem., Int. Ed.* **2006**, *45*, 4926. (g) Tasiopoulos, A. J.; Vinslava, A.; Wernsdorfer, W.; Abboud, K. A.; Christou, G. *Angew. Chem., Int. Ed.* **2004**, *43*, 2117.

(8) (a) Friedman, J. R.; Sarachik, M. P.; Tejada, J.; Ziolo, R. *Phys. Rev. Lett.* **1996**, *76*, 3830. (b) Chakov, N. E.; Lee, S. C.; Harter, A. G.; Kuhns, P. L.; Reyes, A. P.; Hill, S. O.; Dalal, N. S.; Wernsdorfer, W.; Abboud, K. A.; Christou, G. *J. Am. Chem. Soc.* **2006**, *128*, 6975. (c) Hill, S.; Anderson, N.; Wilson, A.; Takahashi, S.; Chakov, N. E.; Murugesu, M.; North, J. M.; Dalal, N. S.; Christou, G. *J. Appl. Phys.* **2005**, *97*, 10M510. (d) Wernsdorfer, W.; Murugesu, M.; Christou, G. *Phys. Rev. Lett.* **2006**, *96*, 057208.

(9) (a) Sessoli, R.; Tsai, H. L.; Schake, A. R.; Wang, S. Y.; Vincent, J. B.; Folting, K.; Gatteschi, D.; Christou, G.; Hendrickson, D. N. *J. Am. Chem. Soc.* **1993**, *115*, 1804. (b) Boskovic, C.; Pink, M.; Huffman, J. C.; Hendrickson, D. N.; Christou, G. *J. Am. Chem. Soc.* **2001**, *123*, 9914. (c) Soler, M.; Artus, P.; Folting, K.; Huffman, J. C.; Hendrickson, D. N.; Christou, G. *Inorg. Chem.* **2001**, *40*, 4902. (d) Artus, P.; Boskovic, C.; Yoo, J.; Streib, W. E.; Brunel, L. C.; Hendrickson, D. N.; Christou, G. *Inorg. Chem.* **2001**, *40*, 4199.

(10) (a) Schake, A. R.; Tsai, H.-L.; de Vries, N.; Webb, R. J.; Folting, K.; Hendrickson, D. N.; Christou, G. *J. Chem. Soc., Chem. Commun.* **1992**, 181. (b) Eppley, H. J.; Tsai, H. L.; Devries, N.; Folting, K.; Christou, G.; Hendrickson, D. N. *J. Am. Chem. Soc.* **1995**, *117*, 301.

(11) (a) Kuroda-Sowa, T.; Nakano, M.; Christou, G.; Hendrickson, D. N. *Polyhedron* **2001**, *20*, 1529. (b) Kuroda-Sowa, T.; Lam, M.; Rheingold, A. L.; Frommen, C.; Reiff, W. M.; Nakano, M.; Yoo, J.; Maniero, A. L.; Brunel, L. C.; Christou, G.; Hendrickson, D. N. *Inorg. Chem.* **2001**, *40*, 6469. (c) Kuroda-Sowa, T.; Nogami, T.; Konaka, H.; Maekawa, M.; Munakata, M.; Miyasaka, H.; Yamashita, M. *Polyhedron* **2003**, *22*, 1795.

(12) Aubin, S. M. J.; Sun, Z. M.; Pardi, L.; Krzystek, J.; Folting, K.; Brunel, L. C.; Rheingold, A. L.; Christou, G.; Hendrickson, D. N. *Inorg. Chem.* **1999**, *38*, 5329. (b) Takeda, K.; Awaga, K. *Phys. Rev. B* **1997**, *56*, 14560. (c) Wernsdorfer, W.; Chakov, N. E.; Christou, G. *Phys. Rev. Lett.* **2005**, *95*, 037203.

description, and the spin was found to be $S = 10$, the same as that of the $Mn_{12}$ parent compound.

The above efforts had thus provided the $Mn_{12}$ family of SMMs in three oxidation states, providing a wealth of comparative chemical and physical data. So much so that it was considered desirable to extend this family to a fourth oxidation level if at all possible. The three-electron reduction of $Mn_{12}$ complexes is in fact observable in the cyclic voltammetry,[13b] and so we decided to pursue the generation and isolation of this oxidation state. This effort has proved successful, and we herein report the synthesis and characterization of the $[Mn_{12}]^{3-}$ salts $(NPr^n_4)_3[Mn_{12}O_{12}(O_2CCHCl_2)_{16}(H_2O)_4]$ and $(NMe_4)_3[Mn_{12}O_{12}(O_2CCHCl_2)_{16}(H_2O)_4]$.

## Experimental Section

**Syntheses.** All manipulations were performed under aerobic conditions using materials as received, unless otherwise noted. $[Mn_{12}O_{12}(O_2CCHCl_2)_{16}(H_2O)_4]$ (**1**) was prepared as described elsewhere.[13b]

**$(NPr^n_4)[Mn_{12}O_{12}(O_2CCHCl_2)_{16}(H_2O)_4]$ (2).** Solid $NPr^n_4I$ (0.03 g, 0.1 mmol) was added to a stirred dark brown solution of complex **1** (0.30 g, 0.10 mmol) in MeCN (15 mL). The resulting solution was stirred for 4 h with no noticeable color change. After 4 h, hexanes (20 mL) were added, causing the formation of two phases, and the mixture was shaken to facilitate the extraction of $I_2$ into the hexanes phase. The hexanes layer was then removed, and the extraction process was repeated a few more times until the hexanes layer was colorless. The two layers were then separated, and the MeCN solution was evaporated to dryness. The residue was dissolved in MeCN (10 mL), and $Et_2O$/hexanes (1:1 v/v, 20 mL) was added. The resulting microcrystalline product was isolated and dried in vacuo. Yield, 70%. Anal. Calcd (Found) for **2**·MeCN ($C_{46}H_{55}N_2Mn_{12}O_{48}Cl_{32}$): C, 17.28 (17.60); H, 1.73 (1.62); N, 0.87 (0.53).

**$(NPr^n_4)_2[Mn_{12}O_{12}(O_2CCHCl_2)_{16}(H_2O)_4]$ (3).** Complex **3** was synthesized following the same procedure as for complex **2**, except that 2 equiv of $NPr^n_4I$ (0.06 g, 0.2 mmol) were employed, and the reaction mixture was stirred for 10 h. Yield, 65%. Anal. Calcd (Found) for **3**·MeCN ($C_{58}H_{83}N_3Mn_{12}O_{48}Cl_{32}$): C, 20.59 (20.82); H, 2.47 (2.26); N, 1.24 (0.88).

**$(NPr^n_4)_3[Mn_{12}O_{12}(O_2CCHCl_2)_{16}(H_2O)_4]$ (4).** Complex **4** was synthesized following the same procedure as for complex **2**, except that 3 equiv of $NPr^n_4I$ (0.09 g, 0.3 mmol) was employed, the reaction mixture was stirred for 40 h, and the product was not recrystallized. Yield, 85%. Anal. Calcd (Found) for **4** ($C_{68}H_{108}N_3Mn_{12}O_{48}Cl_{32}$): C, 23.14 (22.85); H, 3.08 (2.78); N, 1.19 (1.16).

**$(NMe_4)_3[Mn_{12}O_{12}(O_2CCHCl_2)_{16}(H_2O)_4]$ (5).** Complex **5** was synthesized following the same procedure as for complex **4**, except that 3 equiv of $NMe_4I$ (0.06 g, 0.3 mmol) was employed, and the reaction mixture was stirred for 48 h. Yield, 80%. Anal. Calcd (Found) for **5**·MeCN ($C_{46}H_{63}N_4Mn_{12}O_{48}Cl_{32}$): C, 17.08 (16.92); H, 1.96 (1.90); N, 1.73 (1.78).

**Other Studies.** Elemental analyses (C, H, and N) were preformed at the in-house facilities of the University of Florida, Chemistry Department. Direct current (dc) and alternating current (ac) magnetic susceptibility studies were performed at the University of Florida on a Quantum Design MPMS-XL superconducting quantum interference device (SQUID) susceptometer equipped with a 7 T magnet and operating in the 1.8−300 K range. Samples were restrained in eicosane to prevent torquing. Pascal's constants were used to estimate diamagnetic corrections, which were subtracted from the experimental susceptibility to give the molar paramagnetic susceptibilities ($\chi_M$).

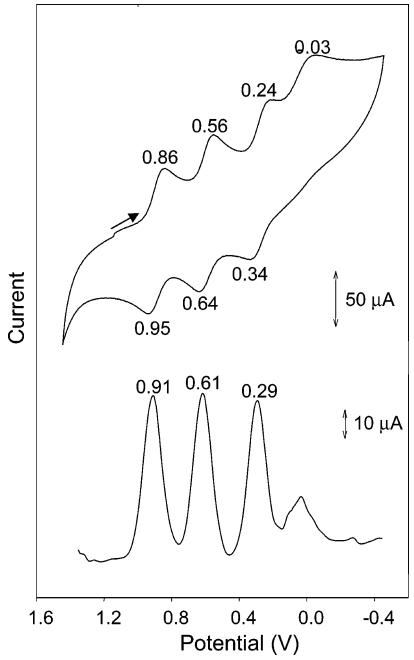


**Figure 1.** CV at 100 mV/s (top) and DPVat 20 mV/s (bottom) for complex **1** in MeCN containing 0.1 M $NBu^n_4PF_6$ as supporting electrolyte. The indicated potentials are vs ferrocene.

## Results and Discussion

**Syntheses.** Electrochemical studies on various $[Mn_{12}O_{12}(O_2CR)_{16}(H_2O)_4]$ complexes have revealed a rich redox chemistry involving several quasi-reversible oxidation and reduction processes.[10,13b,14] In addition, the redox potentials are, as expected, very sensitive to the electron-withdrawing and electron-donating ability of the carboxylate ligand. For example, the value of $E_{1/2}$ (vs ferrrocene) for the first reduction varies by almost a volt from 0.91 V for the R = $CHCl_2$ complex to 0.00 V for the R = $p$-$C_6H_4OMe$ complex. The particularly high electron-withdrawing capability of the R = $CHCl_2$ group, as reflected in the very low p$K_a$ value of 1.48 for $CHCl_2CO_2H$, brought the second reduction potential to 0.61 V (Figure 1), well within the reducing capability of our preferred reducing agent, iodide (0.14 V vs ferrocene in MeCN).[15] This led to the subsequent successful generation and isolation of $(PPh_4)_2[Mn_{12}O_{12}(O_2CCHCl_2)_{16}(H_2O)_4]$ reported elsewhere.[13] Similar results were found for the R = $C_6F_5$ substituent, which has also been used for the synthesis of the two-electron-reduced complex $(NMe_4)_2[Mn_{12}O_{12}(O_2CC_6F_5)_{16}(H_2O)_4]$[16] from the reaction of $[Mn_{12}O_{12}(O_2CC_6F_5)_{16}(H_2O)_4]$ with 2 equiv of $I^-$.

(13) (a) Soler, M.; Chandra, S. K.; Ruiz, D.; Huffman, J. C.; Hendrickson, D. N.; Christou, G. *Polyhedron* **2001**, *20*, 1279. (b) Soler, M.; Wernsdorfer, W.; Abboud, K. A.; Huffman, J. C.; Davidson, E. R.; Hendrickson, D. N.; Christou, G. *J. Am. Chem. Soc.* **2003**, *125*, 3576. (c) Soler, M.; Wernsdorfer, W.; Abboud, K. A.; Hendrickson, D. N.; Christou, G. *Polyhedron* **2003**, *22*, 1777.

(14) Chakov, N. E.; Zakharov, L. N.; Rheingold, A. L.; Abboud, K. A.; Christou, G. *Inorg. Chem.* **2005**, *44*, 4555.

(15) Connelly, N. G.; Geiger, W. E. *Chem. Rev.* **1996**, *96*, 877.

(16) Chakov, N. E.; Soler, M.; Wernsdorfer, W.; Abboud, K. A.; Christou, G. *Inorg. Chem.* **2005**, *44*, 5304.

For the present work, we chose to employ the R = $CHCl_2$ carboxylate complex because it has a particularly well-resolved third one-electron reduction in the cyclic voltammogram (CV) and differential pulse voltammogram (DPV) (Figure 1), and one that is still within the reducing capability of $I^-$. A fourth, clearly irreversible reduction at ~0.1 V represented a potential problem, so we avoided the use of an excess of reducing agent beyond the stoichiometric 3 equiv. Thus, complex **1** was treated with 3 equiv of $NMe_4I$, $NPr^n_4I$, $NBu_4I$, and $PPh_4I$ in MeCN for different lengths of time; the formation of $I_2$ was confirmed by its extraction into a hexane phase. It was found that longer reaction times of ≥40 h were required to give complete conversion of $[Mn_{12}]$ to $[Mn_{12}]^{3,-}$ as established by subsequent characterization of the product; these are much longer times than routinely employed for the $[Mn_{12}]^-$ and $[Mn_{12}]^{2-}$ complexes.[13,16] This suggests that the reduction may involve the binding of $I^-$ to the $[Mn_{12}]^{z-}$ ion prior to electron transfer, which would become disfavored with increasing charge $z-$. Samples of $[Mn_{12}]^{3-}$ salts that were analytically pure (and subsequently shown by magnetism studies to be pure $[Mn_{12}]^{3-}$), were obtained with the $NMe_4^+$ and $NPr^n_4^+$ cations, but we were not satisfied with the purity of the $NBu_4^+$ and $PPh_4^+$ salts. Thus, we used only the $NMe_4^+$ and $NPr^n_4^+$ salts for the detailed studies below. In addition, for better comparisons of $[Mn_{12}]^{z-}$ ($z = 0-3$) complexes with the same cation, we also prepared the $NPr^n_4^+$ salts of the $[Mn_{12}]^-$ and $[Mn_{12}]^{2-}$ complexes. The transformations of **1** into **2**−**4** are summarized by general eq 1, where $z = 1$, 2, or 3.

$$[Mn_{12}O_{12}(O_2CR)_{16}(H_2O)_4] + zI^- \rightarrow [Mn_{12}O_{12}(O_2CR)_{16}(H_2O)_4]^{z-} + z/2I_2 \quad (1)$$

It soon became apparent that the $[Mn_{12}]^{3-}$ anion is far less stable in solution than $[Mn_{12}]^-$ and $[Mn_{12}]^{2-}$. Numerous attempts to grow crystals of a $[Mn_{12}]^{3-}$ salt with various cations and under a number of crystallization conditions were all unsuccessful, giving amorphous powders and/or crystals that turned out to be the $[Mn_{12}]^{2-}$ salt on analysis and magnetic examination. However, in reality a crystal structure would not have told us anything that we did not feel we already knew about the $[Mn_{12}]^{3-}$ anion on the basis of previous observations of what happens to the structure of a $Mn_{12}$ complex on one- and two-electron reduction. The most important structural question about these other complexes had been where does(do) the added electron(s) go, and the answer was on the outer ring of $Mn^{III}$ atoms. This is summarized in Figure 2, which shows the distribution of Mn oxidation states within the $[Mn_{12}O_{12}]$ cores of these compounds. The neutral $Mn_{12}$ (Figure 2, top) has four central $Mn^{IV}$ atoms within a nonplanar ring of eight outer $Mn^{III}$ atoms. The latter divide by symmetry into two classes, and the addition of one or two extra electrons leads to the localization of these electrons onto $Mn^{III}$ atoms of only one class leading to their conversion to $Mn^{II}$, giving $Mn^{IV}_4Mn^{III}_7Mn^{II}$ and $Mn^{IV}_4Mn^{III}_6Mn^{II}_2$ oxidation state descriptions, respectively. This was established from the crystal structures of multiple $[Mn_{12}]^-$ and $[Mn_{12}]^{2-}$ complexes[10−13,16] and is

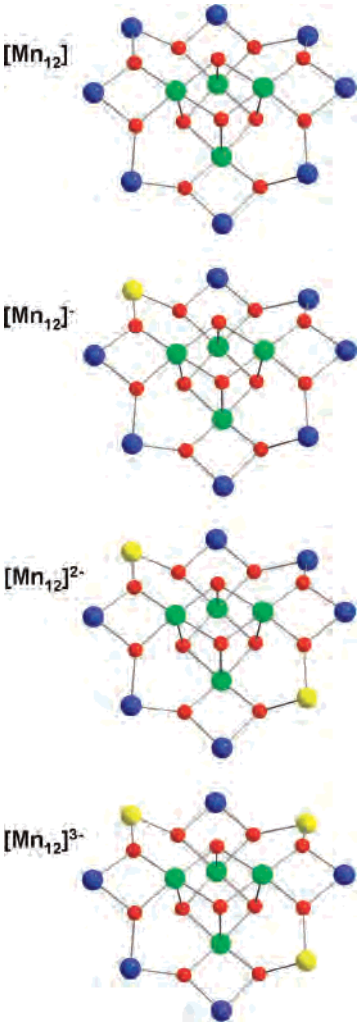


**Figure 2.** The $[Mn_{12}O_{12}]$ cores of **1**−**3** and that proposed for **4**. Color code: $Mn^{IV}$, green; $Mn^{III}$, blue; $Mn^{II}$, yellow, O, red.

shown in the two central structures of Figure 2. This counterintuitive preferential reduction of a $Mn^{III}$ atom rather than a $Mn^{IV}$ atom was rationalized on the basis that the reduction of a central $Mn^{IV}$ atom would convert it into a $Mn^{III}$ atom that would show a characteristic Jahn−Teller distortion, as expected for a high-spin $d^4$ configuration (and exhibited by the outer $Mn^{III}$ atoms). This would introduce strain into the relatively rigid central $Mn_4O_4$ cubane, and so the reduction of an outer $Mn^{III}$ becomes thermodynamically preferred since it causes no significant structural perturbation. We are thus certain that the third added electron in the $[Mn_{12}]^{3-}$ complexes also has added to a formerly $Mn^{III}$ atom of the same symmetry class, giving the $Mn^{IV}_4Mn^{III}_5Mn^{II}_3$ situation depicted in Figure 2 (bottom).

On the basis of the above arguments, the decreased stability of the $[Mn_{12}]^{3-}$ anion in solution compared with the $[Mn_{12}]^{z-}$ ($z = 1$, 2) anions is perhaps not surprising given the now high content of $Mn^{II}$ in a complex that still contains four $Mn^{IV}$ atoms. It is reasonable that such a species would be susceptible to structural degradation initiated perhaps by the lability of the $Mn^{II}$ centers and/or intramolecular redox transitions. This would also rationalize the observation in Figure 1 that the four-electron-reduced species $[Mn_{12}]^{4-}$,

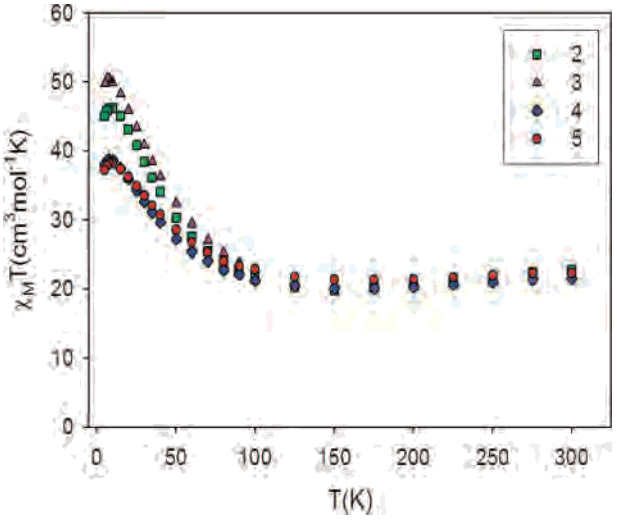


**Figure 3.** Plot of $\chi_M T$ vs $T$ for complexes **2**−**5**.

which would be expected to be $Mn^{IV}_4Mn^{III}_4Mn^{II}_4$, rapidly degrades even on the electrochemical time scale and thus does not show a well-formed peak in the DPV or even a reversible CV wave at the faster CV scan rate.

**Magnetochemistry. dc Magnetic Susceptibility Studies.** Solid-state, variable-temperature dc magnetic susceptibility data in a 0.1 T field and in the 5.0−300 K range were collected on powdered crystalline samples of complexes **2**−**5**, restrained in eicosane to prevent torquing. The obtained data are plotted as $\chi_M T$ vs $T$ in Figure 3. The $\chi_M T$ values for **2**−**5** slowly increase from 22.7, 21.8, 21.5, and 22.3 cm$^3$ K mol$^{-1}$ at 300 K to a maximum of 46.2, 50.1, 38.8, and 38.1 cm$^3$ K mol$^{-1}$ at 10 K, respectively, and then decrease at lower temperatures due to Zeeman effects from the applied field, any weak intermolecular interactions, etc. The $\chi_M T$ vs $T$ profiles of **2** and **3** are essentially identical to those of previously reported $[Mn_{12}]^-$ and $[Mn_{12}]^{2-}$ complexes.[10−13,16] Their maxima of 46.2 and 50.1 cm$^3$ K mol$^{-1}$ at 10 K are indicative of $S = {}^{19}/_2$ and $S = 10$ ground states, respectively, and $g < 2$ as expected for Mn. This is in agreement with the ground states found in previous work for $[Mn_{12}]^-$ and $[Mn_{12}]^{2-}$ complexes.[10−13,16] The calculated, spin-only ($g = 2$) values are 49.9 and 55.0 cm$^3$ K mol$^{-1}$ for $S = {}^{19}/_2$ and $S = 10$, respectively.

The $\chi_M T$ vs $T$ profiles of **4** and **5** are essentially superimposable with each other throughout the whole temperature range and with those of **2** and **3** in the 100−300 K range. Below 100 K, they diverge from those of the latter and reach maxima significantly below those of **2** and **3**. This shows that **4** and **5** are indeed at a different oxidation level from either **2** or **3** and also that they have a smaller ground-state $S$ value than the latter. Remembering that a $Mn^{IV}_4Mn^{III}_5Mn^{II}_3$ complex must have a half-integer ground state, then the $\chi_M T$ maxima at 10 K of 38.8 and 38.1 cm$^3$ K mol$^{-1}$ suggest that **4** and **5** have an $S = {}^{17}/_2$ ground state with $g < 2$; the spin-only ($g = 2$) value is 40.4 cm$^3$ K mol$^{-1}$.

Confirmation of the above preliminary conclusion was sought from fits of magnetization ($M$) data collected on complexes **4** and **5** in the 0.1−4 T and 1.8−10 K ranges. The obtained data are shown as reduced magnetization ($M/N\mu_B$) vs $H/T$ plots in Figure 4, where $N$ is Avogadro's number and $\mu_B$ is the Bohr magneton. The data were fit using the program *MAGNET*[17] by diagonalization of the spin Hamiltonian matrix, assuming that only the ground state is populated, incorporating axial anisotropy ($D\hat{S}_z^2$) and Zeeman terms, and employing a full powder average. The corresponding spin Hamiltonian is given by eq 2

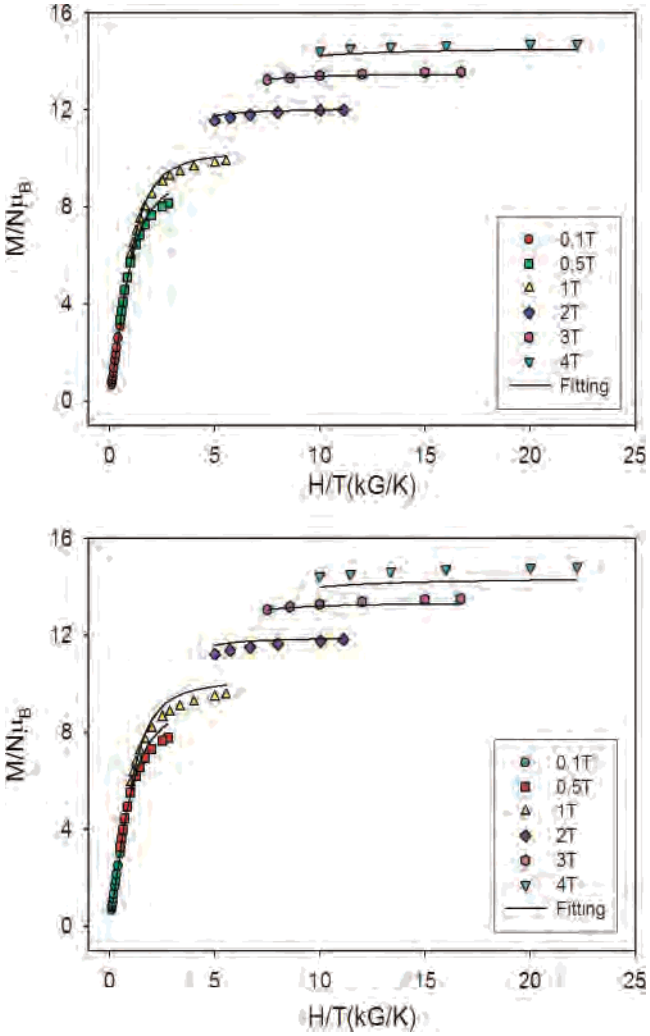


**Figure 4.** Plots of reduced magnetization ($M/N\mu_B$) vs $H/T$ for complex **4** (top) and complex **5** (bottom). The solid lines are the fit of the data; see the text for the fit parameters.

$$\hat{\mathcal{H}} = D\hat{S}_z^2 + g\mu_B\mu_0\hat{S}\cdot H \qquad (2)$$

where $S_z$ is the easy-axis spin operator, $\mu_0$ is the vacuum permeability, and $H$ is the applied field. The last term in eq 2 is the Zeeman energy associated with an applied magnetic field. The best fits for **4** and **5** are shown as the solid lines in Figure 4, and the fit parameters were $S = {}^{17}/_2$, $D = -0.25$ cm$^{-1}$, and $g = 1.91$ for **4** and $S = {}^{17}/_2$, $D = -0.23$ cm$^{-1}$, and $g = 1.90$ for **5**. Fits of the data with $S = {}^{15}/_2$ or ${}^{19}/_2$ gave unreasonable $g$ values of 2.21 and 1.72, respectively and were therefore discounted. For a comparison of the data for complexes with different degrees of reduction but with the

(17) Davidson, E. R. *MAGNET*; Indiana University: Bloomington, IN, 1999.

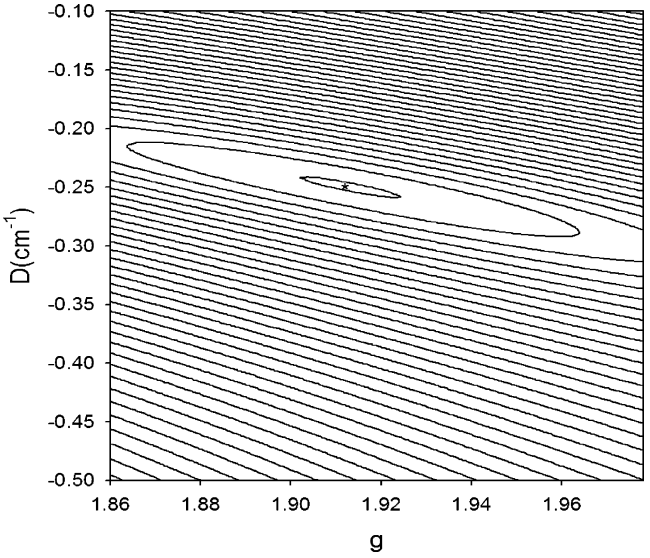


**Figure 5.** 2-D contour plot of the error surface for the $D$ vs $g$ fit for complex **4**.

**Table 1.** Magnetism Data for $[Mn_{12}]^{z-}$ ($z = 0-3$) Complexes **1**−**5**

| | $z = 0$ (**1**) | $z = 1-$ (**2**) | $z = 2-$ (**3**) | $z = 3-$ (**4**) | $z = 3-$ (**5**) |
|---|---|---|---|---|---|
| $S$ | 10 | $^{19}/_2$ | 10 | $^{17}/_2$ | $^{17}/_2$ |
| $g$ | 1.86 | 1.95 | 1.98 | 1.91 | 1.90 |
| $D$/cm$^{-1}$ | −0.45 | −0.35 | −0.28 | −0.25 | −0.23 |
| $D$/K | −0.65 | −0.50 | −0.40 | −0.36 | −0.33 |
| $U$/K[a] | 65 | 45 | 40 | 26 | 24 |

[a] Calculated as $S^2|D|$ for **1** and **3** and as $(S^2 - {}^1/_4)|D|$ for **2**, **4**, and **5**.

same cation, we also collected variable-temperature and variable-field magnetization data for complexes **2** and **3**; the corresponding ($M/N\mu_B$) vs $H/T$ plots and fits are provided in the Supporting Information. The fit parameters were $S = {}^{19}/_2$, $D = -0.35$ cm$^{-1}$, and $g = 1.95$ for **2** and $S = 10$, $D = -0.28$ cm$^{-1}$, and $g = 1.98$ for **3**. The obtained ground-state $S$ values of **2** and **3** are the same as those previously found for several other $[Mn_{12}]^-$ and $[Mn_{12}]^{2-}$ complexes.[10−13,16]

To confirm that the obtained fit minima were the true global minima and to assess the hardness of the fit, a root-mean-square $D$ vs $g$ error surface for the fit was generated for representative complex **4** using the program *GRID*,[18] which calculates the relative difference between the experimental ($M/N\mu_B$)data and those calculated for various combinations of $D$ and $g$. This is shown as a two-dimensional (2-D) contour plot in Figure 5 covering the $D = -0.10$ to $-0.50$ cm$^{-1}$ and $g = 1.86-1.98$ ranges. Only one minimum was observed, and this was a relatively soft minimum; we thus estimate the fitting uncertainties as $D = -0.25 \pm 0.01$ cm$^{-1}$ and $g = 1.91 \pm 0.01$.

**Comparison of the Magnetic Properties of the $[Mn_{12}]^{z-}$ ($z = 0-3$) Family.** The combined results for complexes **2**−**5**, as well as those for neutral complex **1**,[13] are collected in Table 1. Considering first the $S$ values, it is well-known that the spin ground state changes very little on one- and two-electron reduction, from $S = 10$ to $S = {}^{19}/_2$ and then back to $S = 10$ along the series **1** ($z = 0$), **2** ($z = 1$), and **3** ($z = 2$), respectively. Thus, the $Mn_{12}$ core acts almost as a "spin buffer", picking up electrons with little change to the ground-state $S$ value. However, on three-electron reduction to complexes **4** and **5**, there is a more significant change to $S = {}^{17}/_2$. This is no doubt due to the increased $Mn^{II}$ content and the general weakening of many of the exchange interactions in the core. However, the $[Mn_{12}O_{12}]$ core is a complicated one with many symmetry-inequivalent exchange interactions, many of them competing, and it is thus not easy to provide a quantitative rationalization of the $S = {}^{17}/_2$ ground state. Indeed, neither has it been possible in the past to rationalize those of the $[Mn_{12}]^-$ and $[Mn_{12}]^{2-}$ complexes.

The $g$ values given in Table 1 are provided only for completeness and should not be taken as particularly accurate. It is well-known that fits of bulk magnetization data are not a good way to obtain accurate $g$ values. While we prefer to quote the actual values obtained by having the $g$ value as a free parameter, rather than fixing it at a value at or near 2.0, we do not attempt to draw any conclusions from resulting differences in $g$. It would require studies with a more sensitive technique such as EPR spectroscopy to provide more accurate g values.

In contrast to the $S$ value, the axial zero-field splitting parameter $D$ does exhibit a monotonic change with the extent of reduction; there is a clear decrease in $|D|$ with progressive one-electron reduction. This is exactly as expected because the molecular anisotropy, as gauged by the magnitude of $|D|$, is the projection of the single-ion Mn anisotropies onto the molecular anisotropy axis. $Mn^{IV}$ and $Mn^{II}$ are relatively isotropic ions, and the primary contributions to the molecular $D$ value are thus the $Mn^{III}$ ions, which are significantly Jahn−Teller distorted. Since reduction involves the addition of electrons onto formerly $Mn^{III}$ centers, converting them to the $Mn^{II}$ state, the greater the extent of reduction, the fewer the remaining $Mn^{III}$ ions and the lower the molecular anisotropy $|D|$. This assumes that other factors remain the same, such as the overall structure of the $Mn_{12}$ complex and the relative orientation of the $Mn^{III}$ Jahn−Teller axes essentially parallel to the molecular $z$ axis. It should be added that the $D$ values in Table 1 have been obtained by fitting the magnetization data with the rhombic (transverse) zero-field splitting parameter ($E$) fixed at $E = 0$. In fact, these complexes do not have axial symmetry, and $E$ is unlikely to be exactly zero. In our experience, however, bulk magnetization fits are usually not very sensitive to $E$, and the $D$ values in Table 1 are therefore expected to be very reasonable, especially for the assessment of relative magnitudes within a series, as here. Nevertheless, for information purposes, we provide in the Supporting Information the fit of the magnetization data of **4** as a function of $D$ and $E$, with $g$ held constant at 2.0; the fit is shown as a contour plot of the error surface. The best-fit parameters are $D = -0.24$ cm$^{-1}$ and $|E| = 0.065$ cm$^{-1}$. The $D$ value has changed only very slightly from the $-0.25$ cm$^{-1}$ value obtained with $E = 0$, while the nonzero $E$ value is consistent with the low symmetry of a three-electron-reduced $[Mn_{12}]^{3-}$ complex.

The final entries in Table 1 for each compound are the values of the $U$, the anisotropy barrier to magnetization relaxation, whose upper limit is given by $S^2|D|$ and $(S^2 -$

(18) Davidson, E. R. *GRID*; Indiana University: Bloomington, IN, 1999.

$^1/_4)|D|$ for integer and half-integer $S$, respectively. In practice, the true or effective barrier ($U_{eff}$) is smaller than this upper limit because the magnetization vector need not go over the top of the barrier but can tunnel through its upper regions via higher-lying $M_S$ levels. This quantum tunneling of magnetization (QTM) is a characteristic of all SMMs. Since the value of $|D|$ monotonically decreases with reduction, whereas the value of $S$ stays roughly the same or decreases, then it would be expected that $U$ would decrease with reduction, and this is what is indeed seen. The $U$ value for $[Mn_{12}]^{3-}$ complexes **4** and **5**, coming from their $S = {}^{17}/_2$ spin and a $|D|$ value that has been decreased but is still reasonable, is still relatively large, and even a decrease by QTM might still be sufficient for them to function as SMMs. In order to explore whether these $[Mn_{12}]^{3-}$ complexes do in fact exhibit slow relaxation, we investigated their magnetization dynamics using ac susceptibility.

**ac Magnetic Susceptibility Studies.** In ac studies, a weak field (1−5 G) oscillating at a particular frequency, typically up to 1500 Hz, is applied to a sample to probe the dynamics of the magnetization relaxation. If the magnetization vector can relax fast enough to keep up with the oscillating field, then there is no imaginary (out-of-phase) susceptibility signal ($\chi_M''$), and the real (in-phase) susceptibility ($\chi_M'$) is equal to the dc susceptibility. However, if the barrier to magnetization relaxation is significant compared with thermal energy ($kT$), then there is a nonzero $\chi_M''$ signal and the in-phase signal decreases. In addition, the $\chi_M''$ signal will be frequency-dependent. The ac susceptibilities of $[Mn_{12}]^{z-}$ ($z = 0-2$) complexes **1**−**3** have been previously reported, but they were remeasured here for better comparison with those of **4** and **5** under identical conditions.

The ac susceptibilities for complexes **1**−**5** were collected on microcrystalline samples in a 3.5 G ac field, and the obtained data for complexes **4** and **5** at representative frequencies of 50, 250, and 1000 Hz are shown in Figures 6 and 7, respectively, as $\chi_M'T$ vs $T$ and $\chi_M''T$ vs $T$ plots. The in-phase ($\chi_M'T$) ac signal is invaluable as an additional and independent means to determine the ground-state spin of a molecule, without any complications from a dc field.[19] Inspection of Figures 6 and 7 shows that the $\chi_M'T$ values are essentially temperature independent down to ∼5 K, below which they show decreases due to slow relaxation (vide infra). The temperature-independent $\chi_M'T$ shows that only the spin ground state of the molecule is populated at these temperatures and can be used to calculate its $S$ value. The $\chi_M'T$ values of 40.5 and 39.5 cm$^3$ K mol$^{-1}$ for **4** and **5,** respectively, correspond to $S = {}^{17}/_2$ and $g = 2.00$ and $S = {}^{17}/_2$ and $g = 1.98$, in very satisfying agreement with the conclusions from the fits of the dc magnetization data discussed above. Note that for $S = {}^{15}/_2$ or ${}^{19}/_2$ states, a $\chi_M'T$ value of ∼40 cm$^3$ K mol$^{-1}$ would require $g$ values of 2.24 and 1.79, which are unreasonable for Mn. We conclude that

(19) (a) Brechin, E. K.; Sanudo, E. C.; Wernsdorfer, W.; Boskovic, C.; Yoo, J.; Hendrickson, D. N.; Yamaguchi, A.; Ishimoto, H.; Concolino, T. E.; Rheingold, A. L.; Christou, G. *Inorg. Chem.* **2005**, *44*, 502. (b) Sanudo, E. C.; Wernsdorfer, W.; Abboud, K. A.; Christou, G. *Inorg. Chem.* **2004**, *43*, 4137. (c) Murugesu, M.; Habrych, M.; Wernsdorfer, W.; Abboud, K. A.; Christou, G. *J. Am. Chem. Soc.* **2004**, *126*, 4766.

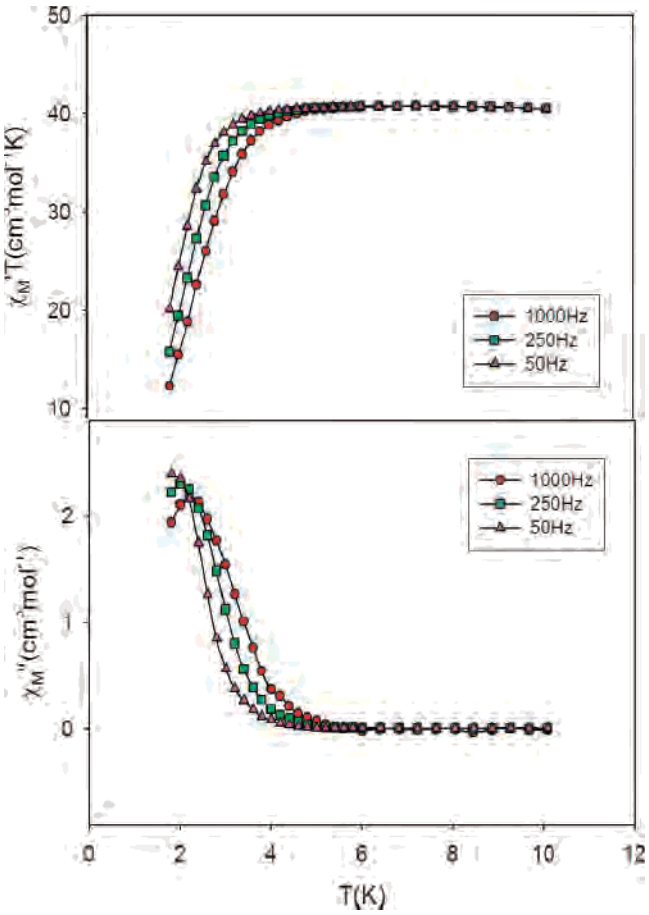


**Figure 6.** Plot of the in-phase ($\chi_M'T$) and out-of-phase ($\chi_M''$) ac susceptibility data for **4**.

$[Mn_{12}]^{3-}$ complexes **4** and **5** are confirmed to possess $S = {}^{17}/_2$ ground states.

Below ∼5 K, the in-phase $\chi_M'T$ signals for **4** and **5** in Figures 6 and 7 exhibit a frequency-dependent decrease concomitant with the appearance of frequency-dependent out-of-phase ($\chi_M''$) signals. This is indicative of the onset of slow magnetization relaxation relative to the ac field, i.e., the magnetization vector can no longer relax fast enough to stay in-phase with the oscillating field. This is the characteristic superparamagnet-like behavior of a SMM and parallels that previously observed for the other oxidation levels of the $[Mn_{12}]^{z-}$ ($z = 0-2$) family. On the basis of the comparative data presented in Table 1, the appearance of the $\chi_M''$ signals at very low temperatures of ∼2.5 K and below are as expected for the barrier to magnetization relaxation in $[Mn_{12}]^{3-}$ complexes, those of **4** and **5** being smaller than those in $[Mn_{12}]^{z-}$ ($z = 0 - 2$) complexes. This is emphasized by the comparative ac data presented in Figure 8, which shows the $\chi_M''$ signals for complexes **1**−**4** at equivalent frequencies of 50, 250, and 1000 Hz. In each case, the $\chi_M''$ signals are frequency-dependent and exhibit a monotonic shift to lower temperatures with increasing reduction: 6−8 K for **1** $[Mn_{12}]$; 4−6 K for **2** $[Mn_{12}]^-$; 2−4 K for **3** $[Mn_{12}]^{2-}$; and ≤2.5 K for **4** $[Mn_{12}]^{3-}$. For better comparisons at identical ac frequencies, the $\chi_M''$ signals for **1**−**4** at 50 and 1000 Hz are plotted together in Figure 9, bottom and top, respectively. A clear shift to lower temperature is seen with

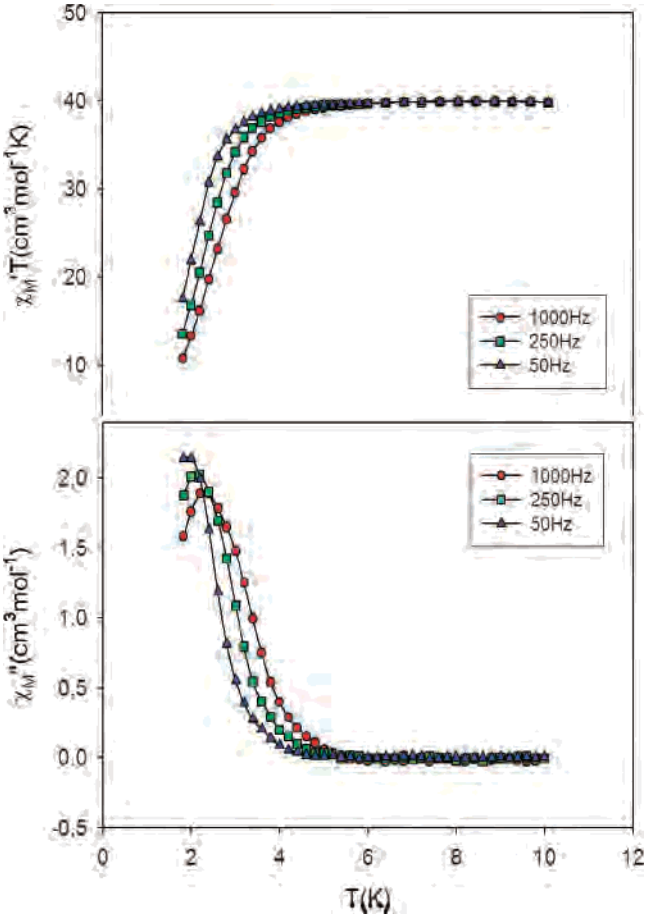


**Figure 7.** Plot of the in-phase ($\chi_M'T$) and out-of-phase ($\chi_M''$) ac susceptibility data for **5**.

each reduction step. The combined data in Figures 8 and 9 are thus perfectly consistent with the conclusions from the data in Table 1 and the discussion above, since the barrier to magnetization relaxation scales with $S^2|D|$, and either one or both of these quantities decrease with each one-electron reduction.

Note that it is not expected that that there should be a linear decrease in barrier with reduction, since there are so many factors that determine the actual magnitude of the true or effective barrier, $U_{eff}$, including $S$, $D$, the rhombic zero-field splitting parameter ($E$), fourth-order spin Hamiltonian parameters, precise QTM rate and tunneling channel (i.e., which $M_s$ levels are involved), spin−phonon coupling strengths, and others. Thus, there are too many parameters that contribute to the observed $U_{eff}$ value to permit a more

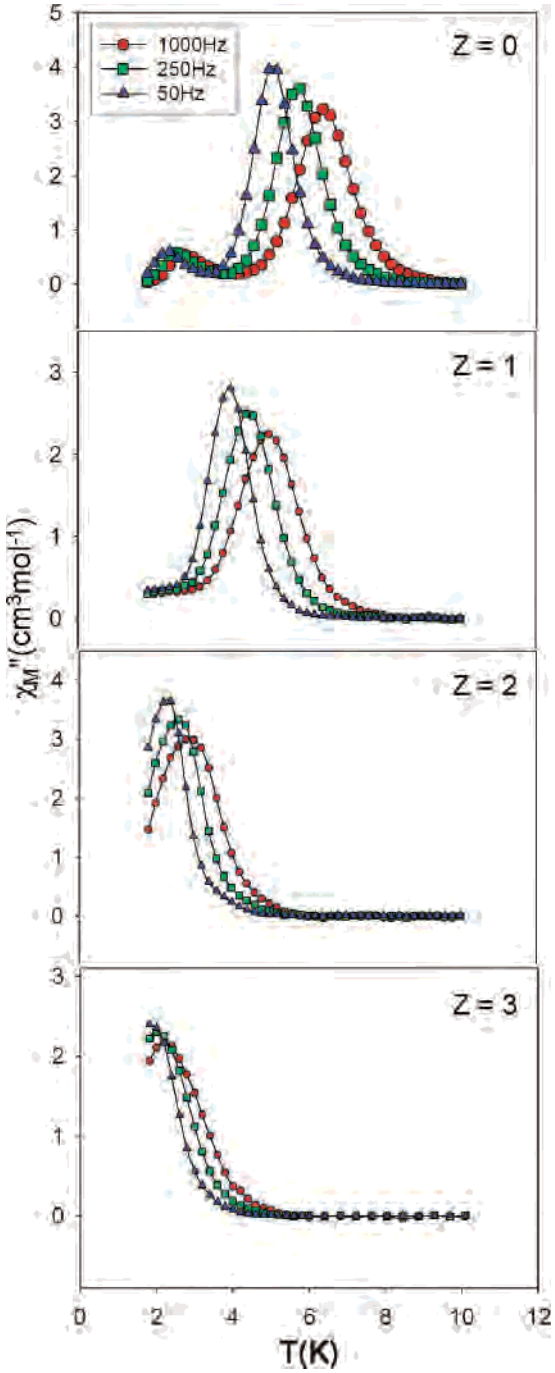


**Figure 8.** $\chi_M''$ vs $T$ plots for $[Mn_{12}]^{z-}$ ($z = 0-3$) complexes **1**−**4** at the indicated frequencies.

quantitative comparison between different oxidation levels. Since we have not been able to obtain single crystals, micro-SQUID hysteresis measurements could not be performed. Note, in addition, that the $\chi_M''$ signals for complex **1** in Figures 8 and 9 also exhibit a weaker signal at lower temperatures, which is due to the faster-relaxing form of neutral $Mn_{12}$ arising from a different Jahn−Teller isomer, i.e., a form in which one of the $Mn^{III}$ Jahn−Teller axes is abnormally oriented toward a bridging oxide ion in the molecule.[20] These isomeric forms are known to possess smaller barriers to magnetization relaxation and thus to exhibit their $\chi_M''$ signals at lower temperatures.

(20) (a) Sun, Z.; Ruiz, D.; Dilley, N. R.; Soler, M.; Ribas, J.; Folting, K.; Maple, M. B.; Christou, G.; Hendrickson, D. N. *Chem. Commun.* **1999**, 1973. (b) Aubin, S. M. J.; Eppley, H. J.; Guzei, I. A.; Folting, K.; Gantzel, P. K.; Rheingold, A. L.; Christou, G.; Hendrickson, D. N. *Inorg. Chem.* **2001**, *40*, 2127. (c) Aubin, S. M. J.; Sun, Z.; Eppley, H. J.; Rumberger, E. M.; Guzei, I. A.; Folting, K.; Gantzel, P. K.; Rheingold, A. L.; Christou, G.; Hendrickson, D. N. *Polyhedron* **2001**, *20*, 1139. (d) Soler, M.; Wernsdorfer, W.; Sun, Z.; Ruiz, D.; Huffman, J. C.; Hendrickson, D. N.; Christou, G. *Polyhedron* **2003**, *22*, 1783. (e) Soler, M.; Wernsdorfer, W.; Sun, Z.; Huffman, J. C.; Hendrickson, D. N.; Christou, G. *Chem. Commun.* **2003**, 2672. (f) Zhao, H. H.; Berlinguette, C. P.; Bacsa, J.; Prosvirin, A. V.; Bera, J. K.; Tichy, S. E.; Schelter, E. J.; Dunbar, K. R. *Inorg. Chem.* **2004**, *43*, 1359.

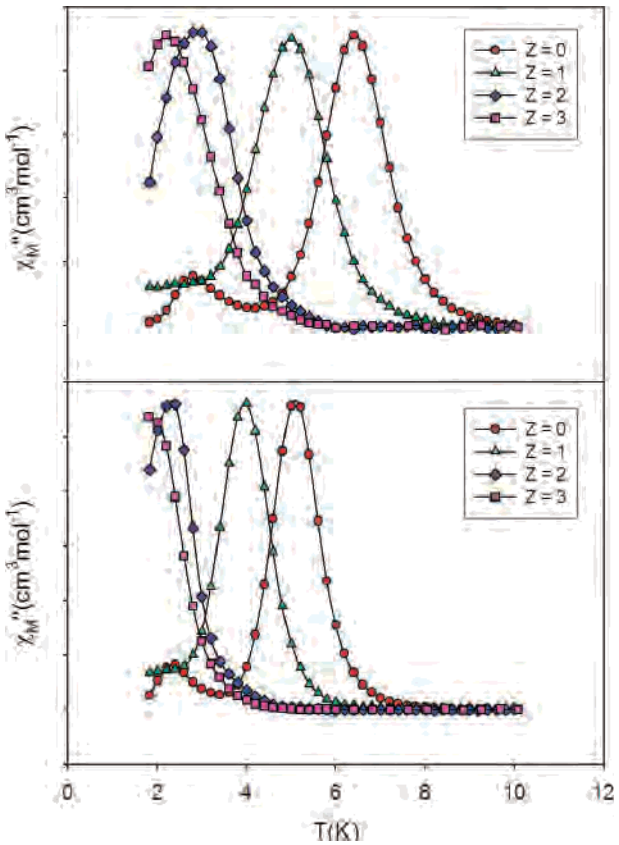


**Figure 9.** Comparison of the $\chi_M''$ vs $T$ plots for $[Mn_{12}]^{z-}$ ($z = 0-3$) at 1000 Hz (top) and 50 Hz (bottom).

## Conclusions

The $Mn_{12}$ family of SMMs has been successfully extended to four isolated oxidation states by the three-electron reduction of $[Mn_{12}O_{12}(O_2CCHCl_2)_{16}(H_2O)_4]$ to $(NR_4)_3[Mn_{12}O_{12}(O_2CCHCl_2)_{16}(H_2O)_4]$ (R = Me, $Pr^n$) with $NR_4I$. The $[Mn_{12}]^{3-}$ complexes are unstable in solution, which has prevented us from obtaining crystals suitable for X-ray crystallography, but this is not unduly disappointing because it is clear on the basis of the structural characterization of the three other $Mn_{12}$ oxidation states that the third electron will have added to an outer, formerly $Mn^{III}$ ion, giving a $Mn^{IV}_4Mn^{III}_5Mn^{II}_3$ trapped-valence situation. We do not believe it will be possible to extend the $Mn_{12}$ family of SMMs to five members by four-electron reduction, given the marked instability demonstrated by the putative $[Mn_{12}]^{4-}$ species in the electrochemical studies.

The $[Mn_{12}]^{3-}$ complexes **4** and **5** both possess a half-integer $S = {}^{17}/_2$ ground state and a $|D|$ value smaller than that for the $[Mn_{12}]^{2-}$ complex **3**, which supports the above assertion that the third added electron is localized on a formerly $Mn^{III}$ ion, since the Jahn−Teller-distorted $Mn^{III}$ ions are the primary source of the molecular anisotropy. As a result of the decreased $S$ and $D$ values relative to those of the other $Mn_{12}$ oxidation states, the barrier to magnetization relaxation $U$ is also smaller than for the other oxidation states but is still sufficient to yield out-of-phase ($\chi_M''$) ac susceptibility signals indicative of slow magnetization relaxation. Thus, we conclude that the $[Mn_{12}]^{3-}$ complexes **4** and **5** are SMMs. Note that the observation of $\chi_M''$ signals is indicative of a SMM but not normally sufficient proof of one. In this case, however, the well-established fact that the $\chi_M''$ ac signals for the other $Mn_{12}$ oxidation states are correctly identifying SMMs, as proven by single-crystal hysteresis studies, leaves little doubt that these same signals for the $[Mn_{12}]^{3-}$ complexes **4** and **5** are also due to SMMs. Thus, although we do not have single crystals with which to carry out micro-SQUID studies down to 0.04 K to observe magnetization hysteresis loops for **4** and **5**, there seems little doubt that the available data are indicating that the $Mn_{12}$ family of SMMs now spans four isolated oxidation levels.

**Acknowledgment.** This work was supported by the National Science Foundation (CHE-0414555).

**Supporting Information Available:** Fits of reduced magnetization ($M/N\mu_B$) vs $H/T$ data for complexes **2** and **3** and a $D$ vs $E$ error surface for the fit of the reduced magnetization data for **4**. This material is available free of charge via the Internet at http://pubs.acs.org.

IC7015758